Thermal energy harvesting to power a battery-less node of a wireless sensor network

Sofía Boselli
Instituto de Ingeniería Eléctrica
Universidad de la República
Montevideo, Uruguay
sofiboselli@hotmail.com

Romina Gaudio
Instituto de Ingeniería Eléctrica
Universidad de la República
Montevideo, Uruguay
rominagaudiocouselo@gmail.com

María Pía Grilli
Instituto de Ingeniería Eléctrica
Universidad de la República
Montevideo, Uruguay
piagrilli23@gmail.com

Fernando Silveira
Instituto de Ingeniería Eléctrica
Universidad de la República
Montevideo, Uruguay
silveira@fing.edu.uy

Mariana Siniscalchi
Instituto de Ingeniería Eléctrica
Universidad de la República
Montevideo, Uruguay
msiniscalchi@fing.edu.uy

***Abstract*—A commercial Peltier cell is experimentally characterized working as a thermoelectric generator for small temperature differences between 1°C and 4°C. The method proposed, consisting of simple experiments together with the model used, can be applied to characterize other thermoelectric generators for similar applications. The measurement results of the output voltage of the Peltier cell for a given resistive load, aid the designer of the energy harvesting circuit to fulfill the specifications of the particular application. A system is implemented to show the feasibility of having a small wearable Peltier cell as the only source of power for a wireless sensor node. The node is IEEE 802.15.4 compliant and transmits three messages every 10 min. In order to adapt the voltage level provided by the Peltier cell to supply the node, an energy harvesting circuit is built based on an off-the-shelf DC-DC converter.**

***Index Terms*—TEG, wireless sensor, DC-DC converter, harvesting circuit**

I. Introduction

Peltier cells are commonly used for cooling and heating, by means of providing a temperature difference between its two surfaces when supplied with a power source. Here, the Peltier cell is used the other way around, meaning that a voltage difference is generated when a temperature difference is applied between the surfaces of the cell, due to the Seebeck effect [1]. For instance, a thermoelectric generator (TEG) patch worn on the skin may provide a 2 to 5°C temperature difference, enabling thermal energy harvesting [2].

This source of energy is environmentally friendly because it is built with non-polluting materials, it is noiseless and has a long service life. Moreover, the Peltier cell is portable, making it suitable for mobile systems, such as wearable medical devices and wireless sensor networks. As a consequence of its primary use being heating and cooling, the manufacturers datasheets [3] lack information on the cell used as a TEG and its performance for temperature differences below 5°C.

Hence, some Peltier cells have been characterized operating as a TEG [4]–[6], by means of applying a temperature difference between the two surfaces of the cell and measuring the output voltage. However, some works lack results for temperature differences below 10°C [5] and 20°C [4].

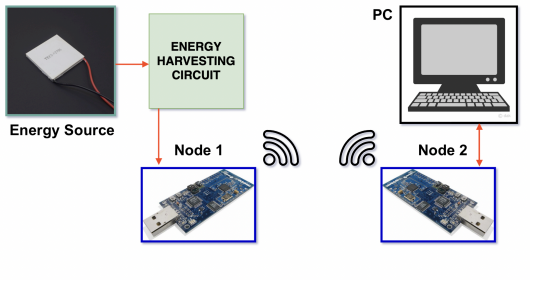

Fig. 1. Diagram of the proposed system to show the viability of energy harvesting.

The performance for temperature differences below 5°C is obtained experimentally for a Peltier cell suitable for energy harvesting applications [3] and the results are presented herein.

An energy harvesting system is built to show the feasibility of using the TEG as the only source of energy in the context of a wireless sensor network application. A diagram of the system is shown in Fig. 1.

The energy harvested with the TEG is converted by means of a harvesting circuit board with a DC-DC converter based on an LTC3108-1 [7]. This DC-DC converter operates with an input voltage as low as 20 mV and can provide output voltages between 2.5 V and 5 V.

A node of a wireless sensor network is supplied with the output voltage of the harvesting circuit. The node is a ”Tmote Sky” [8] based on Texas Instrument’s MSP430 microcontroller with a clock frequency of 8 MHz, 48 KB of flash, 10 KB of RAM and a CC2420 radio that complies with the IEEE 802.15.4 standard [9]. This node sends messages periodically to another node connected to a computer.

The paper is organized as follows. First, it is briefly reviewed the operation of a Peltier cell working as a TEG and the model used is presented. A TEG is experimentally characterized to obtain the output voltage as a function of the temperature difference. Then, the design of the energy

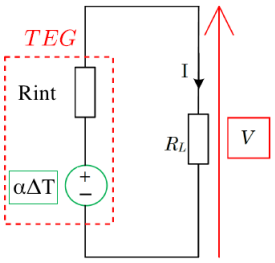

Fig. 2. TEG model used to calculate the coefficient α and the internal resistance R_{int}.

harvesting circuit is presented to fulfill the requirements of the proposed application to wireless sensor networks. The experimental results of the energy harvesting circuit and the whole system are presented and finally some conclusions are drawn.

II. A Peltier Cell to Harvest Thermal Energy

A. Principle of operation and modeling

TEG sources are composed of many thermocouples connected electrically in series and thermally in parallel [1]. Due to the Seebeck effect the voltage difference across the cell is proportional to the temperature difference.

The TEG is modeled, as shown in Fig. 2, as a voltage source dependent on the temperature difference ΔT in series with an internal resistance R_{int}. A load resistance R_L is connected to the TEG. Thus, the voltage V across the TEG is [10]

$$V = \alpha \Delta T \left(\frac{R_L}{R_{int} + R_L} \right), \tag{1}$$

where α is the number of the internal thermocouples times the Seebeck coefficient of each thermocouple.

B. Experimental characterization

The following experiment is conducted in order to find the values of α and R_{int} of the TEG [3].

The set-up shown in Fig. 3 consists of two water baths at different temperatures. Aluminum containers are used to enhance the temperature conductivity. Each container faces one side of the TEG and thermal paste is used to increase conductivity. The containers are filled with water, one at room temperature and the other at approximately 5 °C above room temperature. A multimeter Agilent 34410A [11] connected to the cell measures the voltage difference across the TEG and transmits the data via USB to the computer. The voltage measurements are automatically made every 15 seconds using a Matlab script to control the instruments.

The experiment is carried out for different values of load resistance R_L. First, it is done with $R_L = 6.2\,\Omega$, since it is close to the value of the input resistance of the circuit that will be connected to the TEG to ultimately supply a wireless sensor node. Then, the experiment is repeated with $R_L = 200\,\text{k}\Omega$, to have a different set of measurements to verify the results. Finally, it is repeated in open circuit ($R_L = \infty$), as it upper bounds the voltage that may be generated.

As each experiment takes several hours, the ambient temperature changes, so the bath at ambient temperature is monitored

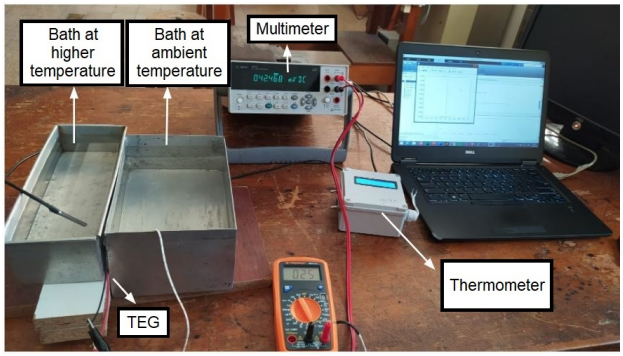

Fig. 3. Experimental setup to monitor the temperature variation in the baths and the voltage generated by the TEG.

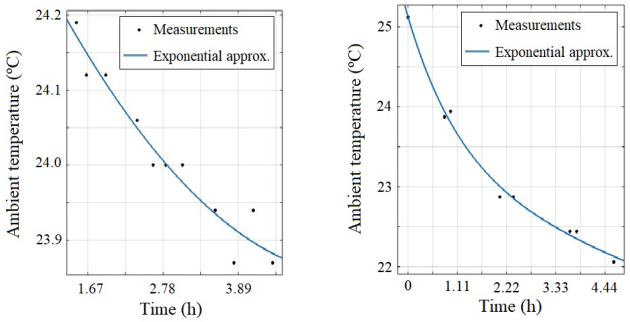

(a) (b)

Fig. 4. Variation of the bath's temperature at ambient temperature with (a) $R_L = 200\,\text{k}\Omega$ and (b) $R_L = 6.2\,\Omega$.

every 10 min. The other bath diminishes its temperature fast, so it is monitored by means of a sensor controller by an Arduino Uno [12] that measures the temperature and sends it to the PC.

In order to correct the temperature difference between the baths taking into account the ambient temperature variation, the latter can be expressed as

$$T(t) = T_a + (T_0 - T_a)e^{-kt}, \tag{2}$$

where T_a is the ambient temperature, T_0 the initial temperature and k a constant. The ambient temperature measurement results are presented in Figs. 4a and 4b for one of the repetitions of the experiment with $R_L = 6.2\,\Omega$ and $R_L = 200\,\text{k}\Omega$, respectively. The variation of the ambient temperature during the experiments in open circuit is negligible, as it is less than 0.5°C. The data is fitted to an exponential, following (2). As a result, the error due to the ambient temperature variation is around 10% of the maximum temperature difference.

The resolution of the thermometer is obtained considering the uncertainty of its temperature sensor resulting in 0.7 °C.

The measurements results of the voltage obtained from the TEG, including the corrections, are shown in Fig. 5. The experiment is repeated in the same apparent conditions, resulting in several sets of data plotted in different colors.

By inspecting (1) it is seen that α is the slope of voltage V vs the temperature difference for $R_L = \infty$. Therefore, α is obtained as the average of the least square approximation of the red and blue sets of results in Fig. 5c. The

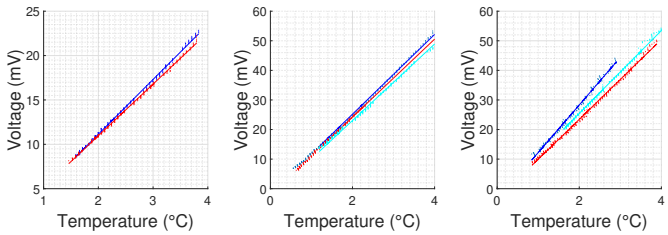

Fig. 5. Voltage supplied by the TEG as a function of the temperature difference applied on both sides of the cell at different loads: a) $R_L = 6.2\,\Omega$ b) $R_L = 200\,\text{k}\Omega$ c) $R_L = \infty$. The dots represent measurements and the lines represent least squares approximation. Each color line corresponds to one repetition of the experiment.

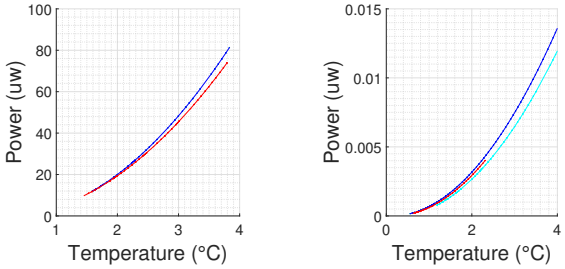

Fig. 6. Power vs. Temperature difference. Power delivered by the Peltier cell for different R_L load resistors: a) $R_L = 6.2\,\Omega$ b)$R_L = 200\,\text{k}\Omega$. The dots represent measurements and the lines represent least squares approximation. Each color line corresponds to one repetition of the experiment.

sky-blue set is disregarded because the ambient temperature fluctuates more during the particular experiment. The result is $\alpha = 13.7\,\text{mV}/^\circ\text{C}$.

The internal resistance of the TEG R_{int} can be obtained from (1) as

$$R_{int} = R_L\,(\alpha/\beta - 1)\,, \tag{3}$$

where the β is the average of the least square approximation for $R_L = 6.2\,\Omega$ in Fig. 5*b*. Thus, $R_{int} = 8\,\Omega$.

As a consequence, the result of R_{int} is much accurate than if it were extracted through the results of the measurements with $R_L = 200\,\text{k}\Omega$. Nevertheless, the results with $R_L = 200\,\text{k}\Omega$ prove useful to verify the value of α, which is 13.19 mV/°C for $R_L = 200\,\text{k}\Omega$. As expected, it is very close to the result obtained in open circuit (13.7 mV/°C).

The power supplied by the TEG is calculated in terms of the measured voltage V as a function of the temperature difference as

$$P(\Delta T) = \frac{V^2\,\Delta T}{R_L} \tag{4}$$

and the results are presented in Fig. 6 for $R_L = 6.2\,\Omega$ and $R_L = 200\,\text{k}\Omega$. Since $R_L = 6.2\,\Omega$ is close to the R_{int} value of $8\,\Omega$, the extracted power in this case is close to the maximum available power, considering the maximum power transfer theorem.

III. Energy Harvesting Circuit

According to the diagram presented in Fig. 1, the energy harvested by means of the TEG is fed to an energy harvesting circuit that converts the output voltage of the TEG to a voltage level suitable for supplying a wireless sensor node in a network.

TABLE I
Current Consumption and Time Intervals

I_{LOAD}: max. peak transmission	17.3 mA
t_{pulse}: duration of the max. peak transmission	4 ms
t: max. duration of one transmission	6.36 s
I_{BURST}: average current of a transmission	1.2 mA
I_Q: current in low power mode (LPM)	75 µA

The program running on the node minimizes the current consumption, by activating its low power mode between periodic transmissions. The operating voltage of the node ranges from 2.1 V to 3.6 V and the current consumption of each mode of operation is listed in Table I. The design of the DC-DC converter takes into consideration these voltage and current requirements of the node, as well as the capabilities of the TEG presented in Section II.

The energy harvesting circuit is implemented based on the DC-DC converter LTC3108-1 [7]. The LTC3108-1 requires some additional components, that are selected following the manufacturer's recommendations. In particular, there are two capacitances that need to be designed very carefully. These are C_{OUT}, the capacitance connected to the output of the converter to prevent the output voltage from falling below a given value, and C_{STORE}, the capacitance where the harvested energy is stored for use during bursts.

Thus, C_{OUT} must be such that [7]

$$C_{OUT} \geq \frac{I_{LOAD}\,t_{pulse}}{\Delta V_{OUT}}, \tag{5}$$

where I_{LOAD} is the maximum current peak supplied to the wireless sensor node, t_{pulse} is the duration of said peak and ΔV_{OUT} is the maximum voltage fall that the capacitor has to endure. Letting V_{OUT} fall 10% below its set point of 3 V, allows for $\Delta V_{OUT} = 0.3\,\text{V}$.

Taking into account the current consumption of the wireless sensor node presented in Table I, results in $C_{OUT} \geq 693\,\mu\text{F}$.

In addition, the equivalent series resistor ESR of C_{OUT} must be low enough to keep $\Delta V_{OUT} = 0.3\,\text{V}$ at all times. Two tantalum capacitors of 470 µF with $ESR = 50\,\text{m}\Omega$ are connected in parallel to implement C_{OUT}, complying with the aforementioned conditions.

On the other hand, C_{STORE} can be calculated as [7]

$$C_{STORE} \geq \frac{[6\mu A + I_Q + (I_{BURST}\,t\,f)]\,T_{STORE}}{5.25\,\text{V} - V_{OUT}}, \tag{6}$$

where I_Q is the mean current between transmissions, I_{BURST} is the current consumption during the transmission, t is the duration of each transmission, f the frequency of the transmissions and T_{STORE} is the time it takes for the capacitor to discharge to 0 V. Here the charging current of the internal LDO regulator of the LTC3108-1 is considered negligible. The frequency of the transmissions is $f = 1.66\,\text{mHz}$, which translates to one transmission of three messages every 10 min. According to the current consumption of the wireless sensor node presented in Table I, it is chosen $C_{STORE} = 470\,\text{mF}$, which provides a reasonable discharging time of 3 h and 9 min.

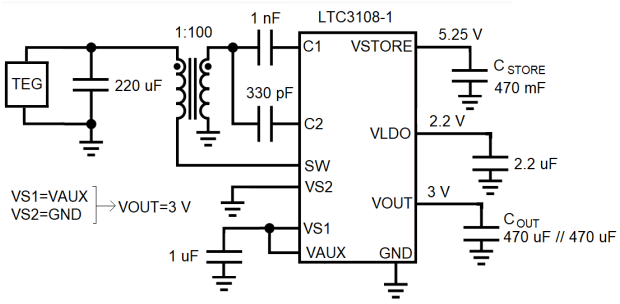

Fig. 7. Circuit schematic of the energy harvesting circuit based on an LTC3108-1 and connected to a TEG, to provide a 3 V supply for a wireless sensor node.

TABLE II
MINIMUM INPUT VOLTAGE FOR DIFFERENT LOAD RESISTORS

$R_{output\,load}$ (MΩ)	∞	8.0	1.02	0.48	0.15
$V_{in\,min}$ (mV)	17	19	20	22	30

Figure 7 shows the circuit schematic with the values selected for all the components.

IV. Experimental Results of the System

It was verified that the minimum input voltage for the LTC3108-1 to work properly is 17 mV, achieved in open circuit. For input voltages below 17 mV, the output voltage falls significantly below the 3 V set point. Table II shows the measurement results of the minimum voltage required at the output of the TEG, depending on the value of the resistive load $R_{output\,load}$ of the harvesting circuit.

Furthermore, to verify that the wireless sensor node can be effectively supplied using the energy harvesting circuit, another node is connected to a computer, acting as a receiver and printing the received messages to the computer terminal. Firstly, a laboratory power supply was used to supply the circuit and the voltage across C_{STORE} was measured. Fig. 8a shows the fabricated PCB and Fig. 8b shows the results for the C_{STORE} voltage when the first node performs transmissions every 3 minutes, for practical reasons in order to save time. At each transmission this voltage decreases and between transmissions C_{STORE} is recharged so that it can continue operating autonomously.

Finally, the harvester system was tested powered by the Peltier cell and the correct operation was verified by receiving a message on the computer.

V. Conclusion

A commercial Peltier Cell was characterized working as a TEG for small temperature differences providing voltages below 50 mV. This enables designing and developing solutions using this TEG in the very low energy harvesting context.

The parameters of the model of the TEG are extracted by means of some simple and effective experiments, for a range of temperatures between 1 °C and 4 °C. This procedure can be extended to other TEGs for similar applications.

An energy harvesting circuit was built to adequate the voltage level to supply a node in a wireless sensor network.

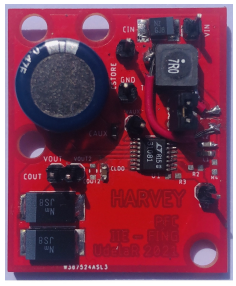

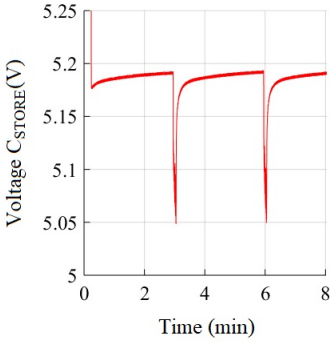

(a) (b)

Fig. 8. (a) Energy harvesting circuit. (b) Measurement results of the voltage of the capacitor C_{STORE} while the circuit is supplied with the Peltier cell and connected to the sensor node. The voltage drops during each transmission and recovers successfully in between.

The system implemented shows the viability of having a small wearable Peltier cell as the only source of power.

Acknowledgment

The authors would like to thank Prof. Nicolás Pérez for his support in the automatic precision temperature measurements, and CSIC, Universidad de la República, for financial support.

Sofía Boselli, Romina Gaudio and María Pía Grilli contributed equally to this paper.

References

[1] N. Jaziri, A. Boughamoura, J. Müller, B. Mezghani, F. Tounsi, and M. Ismail, "A comprehensive review of thermoelectric generators: Technologies and common applications," *Energy Reports*, vol. 6, pp. 264–287, 2020, sI:Energy Storage - driving towards a clean energy future.

[2] H. Bottner, J. Nurnus, A. Gavrikov, G. Kuhner, M. Jagle, C. Kunzel, D. Eberhard, G. Plescher, A. Schubert, and K.-H. Schlereth, "New thermoelectric components using microsystem technologies," *Journal of Microelectromechanical Systems*, vol. 13, no. 3, pp. 414–420, 2004.

[3] *Peltier Module CP85438*, CUI devices, 10 2019. [Online]. Available: https://www.cuidevices.com/product/resource/cp85.pdf

[4] G. Casano and S. Piva, "Experimental investigation of the performance of a thermoelectric generator based on peltier cells," *Experimental Thermal and Fluid Science*, vol. 35, no. 4, pp. 660–669, 2011. [Online]. Available: https://www.sciencedirect.com/science/article/pii/S0894177710002542

[5] L. O. Freire, L. M. Navarrete, B. P. Corrales, and J. N. Castillo, "Efficiency in thermoelectric generators based on peltier cells," *Energy Reports*, vol. 7, pp. 355–361, 2021, 2021 6th International Conference on Advances on Clean Energy Research. [Online]. Available: https://www.sciencedirect.com/science/article/pii/S2352484721007022

[6] S. Dalola, M. Ferrari, V. Ferrari, M. Guizzetti, D. Marioli, and A. Taroni, "Characterization of thermoelectric modules for powering autonomous sensors," *IEEE Transactions on Instrumentation and Measurement*, vol. 58, no. 1, pp. 99–107, 2009.

[7] *LTC3108-1 Datasheet. Ultralow Voltage Step-Up Converter and Power Manager*, Analog Devices, 2019. [Online]. Available: https://www.analog.com/media/en/technical-documentation/data-sheets/31081fb.pdf

[8] *Tmote sky, Ultra low power IEEE 802.15.4 compliant wireless sensor module*, moteiv, 11 2006. [Online]. Available: https://insense.cs.st-andrews.ac.uk/files/2013/04/tmote-sky-datasheet.pdf

[9] "IEEE standard for low-rate wireless networks," *IEEE Std 802.15.4-2015 (Revision of IEEE Std 802.15.4-2011)*, pp. 1–709, April 2016.

[10] S. S. Siouane, S. Jovanovic, and P. Poure, "Equivalent electrical circuits of thermoelectric generators under different operating conditions," *Energies*, vol. 10, p. 386, 03 2017.

[11] *Keysight Technologies 34410A and 34411A Multimeters*, Keysight. [Online]. Available: https://www.keysight.com/us/en/assets/7018-01326/data-sheets/5989-3738.pdf

[12] *Arduino UNO*, Arduino, 2019. [Online]. Available: https://docs.arduino.cc/hardware/uno-rev3